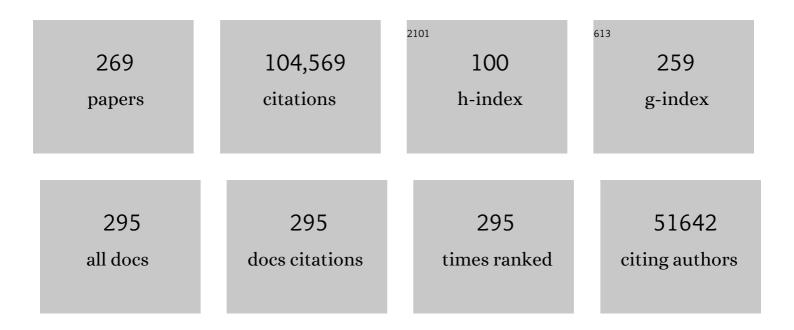
Bruce Fischl Or B Fischl

List of Publications by Year in descending order

Source: https://exaly.com/author-pdf/3550932/publications.pdf Version: 2024-02-01



#	Article	IF	CITATIONS
1	An automated labeling system for subdividing the human cerebral cortex on MRI scans into gyral based regions of interest. Neurolmage, 2006, 31, 968-980.	4.2	10,125
2	Cortical Surface-Based Analysis. NeuroImage, 1999, 9, 179-194.	4.2	9,194
3	Whole Brain Segmentation. Neuron, 2002, 33, 341-355.	8.1	7,404
4	FreeSurfer. NeuroImage, 2012, 62, 774-781.	4.2	6,482
5	The organization of the human cerebral cortex estimated by intrinsic functional connectivity. Journal of Neurophysiology, 2011, 106, 1125-1165.	1.8	6,420
6	Cortical Surface-Based Analysis. NeuroImage, 1999, 9, 195-207.	4.2	5,599
7	The minimal preprocessing pipelines for the Human Connectome Project. NeuroImage, 2013, 80, 105-124.	4.2	4,042
8	Automatically Parcellating the Human Cerebral Cortex. Cerebral Cortex, 2004, 14, 11-22.	2.9	3,657
9	Accurate and robust brain image alignment using boundary-based registration. NeuroImage, 2009, 48, 63-72.	4.2	2,808
10	High-resolution intersubject averaging and a coordinate system for the cortical surface. Human Brain Mapping, 1999, 8, 272-284.	3.6	2,757
11	Automatic parcellation of human cortical gyri and sulci using standard anatomical nomenclature. NeuroImage, 2010, 53, 1-15.	4.2	2,251
12	Within-subject template estimation for unbiased longitudinal image analysis. NeuroImage, 2012, 61, 1402-1418.	4.2	1,925
13	Sequence-independent segmentation of magnetic resonance images. Neurolmage, 2004, 23, S69-S84.	4.2	1,858
14	Thinning of the Cerebral Cortex in Aging. Cerebral Cortex, 2004, 14, 721-730.	2.9	1,556
15	Reliability of MRI-derived measurements of human cerebral cortical thickness: The effects of field strength, scanner upgrade and manufacturer. NeuroImage, 2006, 32, 180-194.	4.2	1,337
16	Meditation experience is associated with increased cortical thickness. NeuroReport, 2005, 16, 1893-1897.	1.2	1,258
17	Transcriptional landscape of the prenatal human brain. Nature, 2014, 508, 199-206.	27.8	1,147
18	Distinct Genetic Influences on Cortical Surface Area and Cortical Thickness. Cerebral Cortex, 2009, 19, 2728-2735.	2.9	1,109

2

#	Article	IF	CITATIONS
19	Reliability in multi-site structural MRI studies: Effects of gradient non-linearity correction on phantom and human data. NeuroImage, 2006, 30, 436-443.	4.2	1,107
20	Highly accurate inverse consistent registration: A robust approach. Neurolmage, 2010, 53, 1181-1196.	4.2	1,099
21	A computational atlas of the hippocampal formation using ex vivo, ultra-high resolution MRI: Application to adaptive segmentation of in vivo MRI. NeuroImage, 2015, 115, 117-137.	4.2	939
22	The Cortical Signature of Alzheimer's Disease: Regionally Specific Cortical Thinning Relates to Symptom Severity in Very Mild to Mild AD Dementia and is Detectable in Asymptomatic Amyloid-Positive Individuals. Cerebral Cortex, 2009, 19, 497-510.	2.9	861
23	Geometrically Accurate Topology-Correction of Cortical Surfaces Using Nonseparating Loops. IEEE Transactions on Medical Imaging, 2007, 26, 518-529.	8.9	848
24	Regionally Localized Thinning of the Cerebral Cortex in Schizophrenia. Archives of General Psychiatry, 2003, 60, 878.	12.3	809
25	Common genetic variants influence human subcortical brain structures. Nature, 2015, 520, 224-229.	27.8	772
26	Cortical Folding Patterns and Predicting Cytoarchitecture. Cerebral Cortex, 2008, 18, 1973-1980.	2.9	691
27	High Consistency of Regional Cortical Thinning in Aging across Multiple Samples. Cerebral Cortex, 2009, 19, 2001-2012.	2.9	580
28	Effects of age on volumes of cortex, white matter and subcortical structures. Neurobiology of Aging, 2005, 26, 1261-1270.	3.1	552
29	Brain morphometry with multiecho MPRAGE. NeuroImage, 2008, 40, 559-569.	4.2	512
30	Automated probabilistic reconstruction of white-matter pathways in health and disease using an atlas of the underlying anatomy. Frontiers in Neuroinformatics, 2011, 5, 23.	2.5	488
31	MRI-derived measurements of human subcortical, ventricular and intracranial brain volumes: Reliability effects of scan sessions, acquisition sequences, data analyses, scanner upgrade, scanner vendors and field strengths. NeuroImage, 2009, 46, 177-192.	4.2	482
32	Spurious group differences due to head motion in a diffusion MRI study. NeuroImage, 2014, 88, 79-90.	4.2	455
33	Cerebral cortex and the clinical expression of Huntington's disease: complexity and heterogeneity. Brain, 2008, 131, 1057-1068.	7.6	438
34	Consistent neuroanatomical age-related volume differences across multiple samples. Neurobiology of Aging, 2011, 32, 916-932.	3.1	437
35	A Role for the Human Dorsal Anterior Cingulate Cortex in Fear Expression. Biological Psychiatry, 2007, 62, 1191-1194.	1.3	425
36	A Generative Model for Image Segmentation Based on Label Fusion. IEEE Transactions on Medical Imaging, 2010, 29, 1714-1729.	8.9	423

#	Article	IF	CITATIONS
37	Cortical Mechanisms Specific to Explicit Visual Object Recognition. Neuron, 2001, 29, 529-535.	8.1	421
38	Toward Implementing an MRI-Based PET Attenuation-Correction Method for Neurologic Studies on the MR-PET Brain Prototype. Journal of Nuclear Medicine, 2010, 51, 1431-1438.	5.0	413
39	Avoiding asymmetry-induced bias in longitudinal image processing. NeuroImage, 2011, 57, 19-21.	4.2	407
40	The Representation of Illusory and Real Contours in Human Cortical Visual Areas Revealed by Functional Magnetic Resonance Imaging. Journal of Neuroscience, 1999, 19, 8560-8572.	3.6	402
41	Head motion during MRI acquisition reduces gray matter volume and thickness estimates. NeuroImage, 2015, 107, 107-115.	4.2	399
42	Automated segmentation of hippocampal subfields from ultraâ€high resolution in vivo MRI. Hippocampus, 2009, 19, 549-557.	1.9	381
43	Laminar analysis of 7T BOLD using an imposed spatial activation pattern in human V1. NeuroImage, 2010, 52, 1334-1346.	4.2	378
44	Thickness of ventromedial prefrontal cortex in humans is correlated with extinction memory. Proceedings of the National Academy of Sciences of the United States of America, 2005, 102, 10706-10711.	7.1	362
45	Focal thinning of the cerebral cortex in multiple sclerosis. Brain, 2003, 126, 1734-1744.	7.6	352
46	Heritability of brain ventricle volume: Converging evidence from inconsistent results. Neurobiology of Aging, 2012, 33, 1-8.	3.1	351
47	Automated MRI measures identify individuals with mild cognitive impairment and Alzheimer's disease. Brain, 2009, 132, 2048-2057.	7.6	341
48	Volumetric navigators for prospective motion correction and selective reacquisition in neuroanatomical MRI. Magnetic Resonance in Medicine, 2012, 68, 389-399.	3.0	338
49	A probabilistic atlas of the human thalamic nuclei combining ex vivo MRI and histology. NeuroImage, 2018, 183, 314-326.	4.2	334
50	Brain Genomics Superstruct Project initial data release with structural, functional, and behavioral measures. Scientific Data, 2015, 2, 150031.	5.3	318
51	Amyloidâ€Î² associated cortical thinning in clinically normal elderly. Annals of Neurology, 2011, 69, 1032-1042.	5.3	306
52	Comprehensive cellularâ€resolution atlas of the adult human brain. Journal of Comparative Neurology, 2016, 524, 3127-3481.	1.6	302
53	Spherical Demons: Fast Diffeomorphic Landmark-Free Surface Registration. IEEE Transactions on Medical Imaging, 2010, 29, 650-668.	8.9	301
54	Statistical analysis of longitudinal neuroimage data with Linear Mixed Effects models. NeuroImage, 2013, 66, 249-260.	4.2	298

#	Article	IF	CITATIONS
55	Extending the Human Connectome Project across ages: Imaging protocols for the Lifespan Development and Aging projects. NeuroImage, 2018, 183, 972-984.	4.2	290
56	Regional white matter volume differences in nondemented aging and Alzheimer's disease. NeuroImage, 2009, 44, 1247-1258.	4.2	267
57	The Dynamics of Cortical and Hippocampal Atrophy in Alzheimer Disease. Archives of Neurology, 2011, 68, 1040.	4.5	267
58	Hierarchical Genetic Organization of Human Cortical Surface Area. Science, 2012, 335, 1634-1636.	12.6	266
59	Permutation Tests for Classification: Towards Statistical Significance in Image-Based Studies. Lecture Notes in Computer Science, 2003, 18, 330-341.	1.3	254
60	Location and spatial profile of categoryâ€specific regions in human extrastriate cortex. Human Brain Mapping, 2006, 27, 77-89.	3.6	249
61	Differential effects of aging and Alzheimer's disease on medial temporal lobe cortical thickness and surface area. Neurobiology of Aging, 2009, 30, 432-440.	3.1	249
62	Evaluating the validity of volume-based and surface-based brain image registration for developmental cognitive neuroscience studies in children 4 to 11years of age. NeuroImage, 2010, 53, 85-93.	4.2	243
63	Evaluation of volume-based and surface-based brain image registration methods. NeuroImage, 2010, 51, 214-220.	4.2	237
64	Widespread Reductions of Cortical Thickness in Schizophrenia and Spectrum Disorders and Evidence of Heritability. Archives of General Psychiatry, 2009, 66, 467.	12.3	235
65	Altered white matter microstructure in the corpus callosum in Huntington's disease: Implications for cortical "disconnection― NeuroImage, 2010, 49, 2995-3004.	4.2	231
66	FastSurfer - A fast and accurate deep learning based neuroimaging pipeline. NeuroImage, 2020, 219, 117012.	4.2	229
67	Accurate prediction of V1 location from cortical folds in a surface coordinate system. NeuroImage, 2008, 39, 1585-1599.	4.2	221
68	Studying neuroanatomy using MRI. Nature Neuroscience, 2017, 20, 314-326.	14.8	220
69	Cortical atrophy is relevant in multiple sclerosis at clinical onset. Journal of Neurology, 2007, 254, 1212-1220.	3.6	208
70	Genetic and environmental influences on the size of specific brain regions in midlife: The VETSA MRI study. NeuroImage, 2010, 49, 1213-1223.	4.2	208
71	Tracking the Roots of Reading Ability: White Matter Volume and Integrity Correlate with Phonological Awareness in Prereading and Early-Reading Kindergarten Children. Journal of Neuroscience, 2013, 33, 13251-13258.	3.6	207
72	Genetic topography of brain morphology. Proceedings of the National Academy of Sciences of the United States of America, 2013, 110, 17089-17094.	7.1	197

#	Article	IF	CITATIONS
73	Atlas Renormalization for Improved Brain MR Image Segmentation Across Scanner Platforms. IEEE Transactions on Medical Imaging, 2007, 26, 479-486.	8.9	193
74	A Surface-based Analysis of Language Lateralization and Cortical Asymmetry. Journal of Cognitive Neuroscience, 2013, 25, 1477-1492.	2.3	188
75	Bayesian segmentation of brainstem structures in MRI. NeuroImage, 2015, 113, 184-195.	4.2	186
76	The Lifespan Human Connectome Project in Aging: An overview. NeuroImage, 2019, 185, 335-348.	4.2	186
77	Cortical surface-based analysis reduces bias and variance in kinetic modeling of brain PET data. Neurolmage, 2014, 92, 225-236.	4.2	179
78	7 Tesla MRI of the ex vivo human brain at 100 micron resolution. Scientific Data, 2019, 6, 244.	5.3	179
79	False positive rates in surface-based anatomical analysis. NeuroImage, 2018, 171, 6-14.	4.2	177
80	On-line automatic slice positioning for brain MR imaging. NeuroImage, 2005, 27, 222-230.	4.2	166
81	Quantitative evaluation of automated skull-stripping methods applied to contemporary and legacy images: Effects of diagnosis, bias correction, and slice location. Human Brain Mapping, 2006, 27, 99-113.	3.6	161
82	Measuring and comparing brain cortical surface area and other areal quantities. NeuroImage, 2012, 61, 1428-1443.	4.2	157
83	Segregation of Somatosensory Activation in the Human Rolandic Cortex Using fMRI. Journal of Neurophysiology, 2000, 84, 558-569.	1.8	156
84	The Association between a Polygenic Alzheimer Score and Cortical Thickness in Clinically Normal Subjects. Cerebral Cortex, 2012, 22, 2653-2661.	2.9	145
85	Mapping an intrinsic MR property of gray matter in auditory cortex of living humans: A possible marker for primary cortex and hemispheric differences. NeuroImage, 2006, 32, 1524-1537.	4.2	144
86	Combined Volumetric and Surface Registration. IEEE Transactions on Medical Imaging, 2009, 28, 508-522.	8.9	144
87	Gray matter myelination of 1555 human brains using partial volume corrected MRI images. NeuroImage, 2015, 105, 473-485.	4.2	141
88	The relationship between diffusion tensor imaging and volumetry as measures of white matter properties. Neurolmage, 2008, 42, 1654-1668.	4.2	136
89	Heritability of Brain Morphology Related to Schizophrenia: A Large-Scale Automated Magnetic Resonance Imaging Segmentation Study. Biological Psychiatry, 2008, 63, 475-483.	1.3	134
90	Brain Structure Correlates of Individual Differences in the Acquisition and Inhibition of Conditioned Fear. Cerebral Cortex, 2011, 21, 1954-1962.	2.9	131

#	Article	IF	CITATIONS
91	Bayesian longitudinal segmentation of hippocampal substructures in brain MRI using subject-specific atlases. NeuroImage, 2016, 141, 542-555.	4.2	130
92	BrainPrint: A discriminative characterization of brain morphology. NeuroImage, 2015, 109, 232-248.	4.2	128
93	Anatomical atlas-guided diffuse optical tomography of brain activation. NeuroImage, 2010, 49, 561-567.	4.2	125
94	A technique for the deidentification of structural brain MR images. Human Brain Mapping, 2007, 28, 892-903.	3.6	124
95	Cortical Thickness Is Influenced by Regionally Specific Genetic Factors. Biological Psychiatry, 2010, 67, 493-499.	1.3	124
96	Thickness of the human cerebral cortex is associated with metrics of cerebrovascular health in a normative sample of community dwelling older adults. NeuroImage, 2011, 54, 2659-2671.	4.2	122
97	Orbitofrontal thickness, retention of fear extinction, and extraversion. NeuroReport, 2005, 16, 1909-1912.	1.2	120
98	A Comparison of Heritability Maps of Cortical Surface Area and Thickness and the Influence of Adjustment for Whole Brain Measures: A Magnetic Resonance Imaging Twin Study. Twin Research and Human Genetics, 2012, 15, 304-314.	0.6	120
99	Connectivity-based segmentation of human amygdala nuclei using probabilistic tractography. Neurolmage, 2011, 56, 1353-1361.	4.2	119
100	Genetic Influences on Cortical Regionalization in the Human Brain. Neuron, 2011, 72, 537-544.	8.1	118
101	Selective increase of cortical thickness in high-performing elderly—structural indices of optimal cognitive aging. Neurolmage, 2006, 29, 984-994.	4.2	112
102	Minute Effects of Sex on the Aging Brain: A Multisample Magnetic Resonance Imaging Study of Healthy Aging and Alzheimer's Disease. Journal of Neuroscience, 2009, 29, 8774-8783.	3.6	111
103	Spatiotemporal linear mixed effects modeling for the mass-univariate analysis of longitudinal neuroimage data. NeuroImage, 2013, 81, 358-370.	4.2	111
104	Prospective motion correction with volumetric navigators (vNavs) reduces the bias and variance in brain morphometry induced by subject motion. NeuroImage, 2016, 127, 11-22.	4.2	109
105	Feasibility of Multi-site Clinical Structural Neuroimaging Studies of Aging Using Legacy Data. Neuroinformatics, 2007, 5, 235-245.	2.8	103
106	Increased sensitivity to effects of normal aging and Alzheimer's disease on cortical thickness by adjustment for local variability in gray/white contrast: A multi-sample MRI study. NeuroImage, 2009, 47, 1545-1557.	4.2	103
107	Locating the functional and anatomical boundaries of human primary visual cortex. NeuroImage, 2009, 46, 915-922.	4.2	98
108	Infant FreeSurfer: An automated segmentation and surface extraction pipeline for T1-weighted neuroimaging data of infants 0–2 years. NeuroImage, 2020, 218, 116946.	4.2	96

#	Article	IF	CITATIONS
109	Cognitive function and brain structure correlations in healthy elderly East Asians. NeuroImage, 2009, 46, 257-269.	4.2	95
110	How to Measure Cortical Folding from MR Images: a Step-by-Step Tutorial to Compute Local Gyrification Index. Journal of Visualized Experiments, 2012, , e3417.	0.3	95
111	Differences in the right inferior longitudinal fasciculus but no general disruption of white matter tracts in children with autism spectrum disorder. Proceedings of the National Academy of Sciences of the United States of America, 2014, 111, 1981-1986.	7.1	95
112	Analysis strategies for high-resolution UHF-fMRI data. NeuroImage, 2018, 168, 296-320.	4.2	95
113	Predicting the location of entorhinal cortex from MRI. NeuroImage, 2009, 47, 8-17.	4.2	94
114	The Cytoarchitecture of Domain-specific Regions in Human High-level Visual Cortex. Cerebral Cortex, 2017, 27, 146-161.	2.9	94
115	Neuroanatomical aging: Universal but not uniform. Neurobiology of Aging, 2005, 26, 1279-1282.	3.1	93
116	Automated MRI measures predict progression to Alzheimer's disease. Neurobiology of Aging, 2010, 31, 1364-1374.	3.1	91
117	Shared genetic risk between corticobasal degeneration, progressive supranuclear palsy, and frontotemporal dementia. Acta Neuropathologica, 2017, 133, 825-837.	7.7	90
118	Salivary cortisol and prefrontal cortical thickness in middle-aged men: A twin study. NeuroImage, 2010, 53, 1093-1102.	4.2	88
119	Genetic and Environmental Contributions to Regional Cortical Surface Area in Humans: A Magnetic Resonance Imaging Twin Study. Cerebral Cortex, 2011, 21, 2313-2321.	2.9	88
120	Cortical Surface Shape Analysis Based on Spherical Wavelets. IEEE Transactions on Medical Imaging, 2007, 26, 582-597.	8.9	87
121	Segmental Brain Volumes and Cognitive and Perceptual Correlates inÂ15-Year-Old Adolescents with Low Birth Weight. Journal of Pediatrics, 2009, 155, 848-853.e1.	1.8	87
122	Blockface histology with optical coherence tomography: A comparison with Nissl staining. NeuroImage, 2014, 84, 524-533.	4.2	87
123	Quantitative comparison of cortical surface reconstructions from MP2RAGE and multi-echo MPRAGE data at 3 and 7T. NeuroImage, 2014, 90, 60-73.	4.2	85
124	The Genetic Association Between Neocortical Volume and General Cognitive Ability Is Driven by Global Surface Area Rather Than Thickness. Cerebral Cortex, 2015, 25, 2127-2137.	2.9	84
125	Effects of registration regularization and atlas sharpness on segmentation accuracy. Medical Image Analysis, 2008, 12, 603-615.	11.6	82
126	Validating atlas-guided DOT: A comparison of diffuse optical tomography informed by atlas and subject-specific anatomies. NeuroImage, 2012, 62, 1999-2006.	4.2	81

#	Article	IF	CITATIONS
127	Predicting the location of human perirhinal cortex, Brodmann's area 35, from MRI. NeuroImage, 2013, 64, 32-42.	4.2	81
128	Is Synthesizing MRI Contrast Useful for Inter-modality Analysis?. Lecture Notes in Computer Science, 2013, 16, 631-638.	1.3	81
129	H.M.'s contributions to neuroscience: A review and autopsy studies. Hippocampus, 2014, 24, 1267-1286.	1.9	80
130	Reduced microstructural integrity of the white matter underlying anterior cingulate cortex is associated with increased saccadic latency in schizophrenia. NeuroImage, 2007, 37, 599-610.	4.2	78
131	Advantages of cortical surface reconstruction using submillimeter 7ÂT MEMPRAGE. NeuroImage, 2018, 165, 11-26.	4.2	76
132	A Genetic Algorithm for the Topology Correction of Cortical Surfaces. Lecture Notes in Computer Science, 2005, 19, 393-405.	1.3	75
133	Accurate nonlinear mapping between MNI volumetric and FreeSurfer surface coordinate systems. Human Brain Mapping, 2018, 39, 3793-3808.	3.6	75
134	Direct visualization of the perforant pathway in the human brain with ex vivo diffusion tensor imaging. Frontiers in Human Neuroscience, 2010, 4, 42.	2.0	74
135	Human Cerebellum: Surface-Assisted Cortical Parcellation and Volumetry with Magnetic Resonance Imaging. Journal of Cognitive Neuroscience, 2003, 15, 584-599.	2.3	70
136	Neural Activity Is Modulated by Trial History: A Functional Magnetic Resonance Imaging Study of the Effects of a Previous Antisaccade. Journal of Neuroscience, 2007, 27, 1791-1798.	3.6	70
137	Abnormal cortical folding patterns within Broca's area in schizophrenia: Evidence from structural MRI. Schizophrenia Research, 2007, 94, 317-327.	2.0	69
138	Selective Disruption of the Cerebral Neocortex in Alzheimer's Disease. PLoS ONE, 2010, 5, e12853.	2.5	69
139	Presence of ApoE ε4 Allele Associated with Thinner Frontal Cortex in Middle Age. Journal of Alzheimer's Disease, 2011, 26, 49-60.	2.6	68
140	Dementia After Moderate-Severe Traumatic Brain Injury: Coexistence of Multiple Proteinopathies. Journal of Neuropathology and Experimental Neurology, 2018, 77, 50-63.	1.7	68
141	Regional cortical thickness matters in recall after months more than minutes. NeuroImage, 2006, 31, 1343-1351.	4.2	66
142	Human cerebral cortex: A system for the integration of volume- and surface-based representations. NeuroImage, 2006, 33, 139-153.	4.2	66
143	Improved tractography alignment using combined volumetric and surface registration. NeuroImage, 2010, 51, 206-213.	4.2	64
144	Cross-validation of serial optical coherence scanning and diffusion tensor imaging: A study on neural fiber maps in human medulla oblongata. NeuroImage, 2014, 100, 395-404.	4.2	63

#	Article	IF	CITATIONS
145	Assessing atrophy measurement techniques in dementia: Results from the MIRIAD atrophy challenge. NeuroImage, 2015, 123, 149-164.	4.2	63
146	A FreeSurfer-compliant consistent manual segmentation of infant brains spanning the 0ââ,¬â€œ2 year age range. Frontiers in Human Neuroscience, 2015, 9, 21.	2.0	60
147	Unsupervised Medical Image Segmentation Based on the Local Center of Mass. Scientific Reports, 2018, 8, 13012.	3.3	59
148	Cortical volume and speed-of-processing are complementary in prediction of performance intelligence. Neuropsychologia, 2005, 43, 704-713.	1.6	58
149	Detailed semiautomated MRI based morphometry of the neonatal brain: Preliminary results. NeuroImage, 2006, 32, 1041-1049.	4.2	58
150	Learning Task-Optimal Registration Cost Functions for Localizing Cytoarchitecture and Function in the Cerebral Cortex. IEEE Transactions on Medical Imaging, 2010, 29, 1424-1441.	8.9	57
151	An MRI-based method for measuring volume, thickness and surface area of entorhinal, perirhinal, and posterior parahippocampal cortex. Neurobiology of Aging, 2009, 30, 420-431.	3.1	56
152	SynthStrip: skull-stripping for any brain image. NeuroImage, 2022, 260, 119474.	4.2	56
153	A tale of two factors: What determines the rate of progression in Huntington's disease? A longitudinal MRI study. Movement Disorders, 2011, 26, 1691-1697.	3.9	55
154	AnatomiCuts: Hierarchical clustering of tractography streamlines based on anatomical similarity. NeuroImage, 2018, 166, 32-45.	4.2	55
155	Morphometricity as a measure of the neuroanatomical signature of a trait. Proceedings of the National Academy of Sciences of the United States of America, 2016, 113, E5749-56.	7.1	53
156	Optical coherence tomography visualizes neurons in human entorhinal cortex. Neurophotonics, 2015, 2, 015004.	3.3	52
157	Joint super-resolution and synthesis of 1Âmm isotropic MP-RAGE volumes from clinical MRI exams with scans of different orientation, resolution and contrast. NeuroImage, 2021, 237, 118206.	4.2	52
158	Cognitive function, P3a/P3b brain potentials, and cortical thickness in aging. Human Brain Mapping, 2007, 28, 1098-1116.	3.6	51
159	Conceptual and Data-based Investigation of Genetic Influences and Brain Asymmetry: A Twin Study of Multiple Structural Phenotypes. Journal of Cognitive Neuroscience, 2014, 26, 1100-1117.	2.3	50
160	as-PSOCT: Volumetric microscopic imaging of human brain architecture and connectivity. Neurolmage, 2018, 165, 56-68.	4.2	50
161	Collaborative computational anatomy: An MRI morphometry study of the human brain via diffeomorphic metric mapping. Human Brain Mapping, 2009, 30, 2132-2141.	3.6	48
162	Joint reconstruction of white-matter pathways from longitudinal diffusion MRI data with anatomical priors. Neurolmage, 2016, 127, 277-286.	4.2	48

#	Article	IF	CITATIONS
163	Comparison of Manual and Automatic Section Positioning of Brain MR Images. Radiology, 2006, 239, 246-254.	7.3	47
164	Genetic patterns of correlation among subcortical volumes in humans: Results from a magnetic resonance imaging twin study. Human Brain Mapping, 2011, 32, 641-653.	3.6	47
165	Markerless highâ€frequency prospective motion correction for neuroanatomical MRI. Magnetic Resonance in Medicine, 2019, 82, 126-144.	3.0	47
166	A probabilistic template of human mesopontine tegmental nuclei from in vivo 7 T MRI. NeuroImage, 2018, 170, 222-230.	4.2	45
167	MarkVCID cerebral small vessel consortium: II. Neuroimaging protocols. Alzheimer's and Dementia, 2021, 17, 716-725.	0.8	45
168	HyperMorph: Amortized Hyperparameter Learning for Image Registration. Lecture Notes in Computer Science, 2021, , 3-17.	1.3	45
169	Intrinsic Functional Connectivity of the Brain in Adults with a Single Cerebral Hemisphere. Cell Reports, 2019, 29, 2398-2407.e4.	6.4	44
170	Differing neuropsychological and neuroanatomical correlates of abnormal reading in early-stage semantic dementia and dementia of the Alzheimer type. Neuropsychologia, 2005, 43, 833-846.	1.6	43
171	Atlas Generation for Subcortical and Ventricular Structures With Its Applications in Shape Analysis. IEEE Transactions on Image Processing, 2010, 19, 1539-1547.	9.8	43
172	Insight into the fundamental trade-offs of diffusion MRI from polarization-sensitive optical coherence tomography in ex vivo human brain. NeuroImage, 2020, 214, 116704.	4.2	42
173	SynthMorph: Learning Contrast-Invariant Registration Without Acquired Images. IEEE Transactions on Medical Imaging, 2022, 41, 543-558.	8.9	42
174	White matter signal abnormality quality differentiates mild cognitive impairment that converts to Alzheimer's disease from nonconverters. Neurobiology of Aging, 2015, 36, 2447-2457.	3.1	41
175	Characterizing the optical properties of human brain tissue with high numerical aperture optical coherence tomography. Biomedical Optics Express, 2017, 8, 5617.	2.9	41
176	Intracortical smoothing of small-voxel fMRI data can provide increased detection power without spatial resolution losses compared to conventional large-voxel fMRI data. NeuroImage, 2019, 189, 601-614.	4.2	41
177	Cognitive reserve moderates the association between hippocampal volume and episodic memory in middle age. Neuropsychologia, 2013, 51, 1124-1131.	1.6	38
178	Impact of MRI head placement on glioma response assessment. Journal of Neuro-Oncology, 2014, 118, 123-129.	2.9	38
179	Unsupervised Deep Learning for Bayesian Brain MRI Segmentation. Lecture Notes in Computer Science, 2019, 11766, 356-365.	1.3	38
180	Spherical Demons: Fast Surface Registration. Lecture Notes in Computer Science, 2008, 11, 745-753.	1.3	38

#	Article	IF	CITATIONS
181	A magnetic resonance imaging study of cortical thickness in animal phobia. Biological Psychiatry, 2004, 55, 946-952.	1.3	37
182	MRI parcellation of ex vivo medial temporal lobe. NeuroImage, 2014, 93, 252-259.	4.2	37
183	Changes in Cerebral Cortex of Children Treated for Medulloblastoma. International Journal of Radiation Oncology Biology Physics, 2007, 68, 992-998.	0.8	36
184	The Intrinsic Shape of Human and Macaque Primary Visual Cortex. Cerebral Cortex, 2008, 18, 2586-2595.	2.9	35
185	Mapping the subcortical connectivity of the human default mode network. NeuroImage, 2021, 245, 118758.	4.2	34
186	Localizing the human primary auditory cortex in vivo using structural MRI. NeuroImage, 2014, 93, 237-251.	4.2	33
187	Fullyâ€∎utomated, multiâ€stage hippocampus mapping in very mild Alzheimer disease. Hippocampus, 2009, 19, 541-548.	1.9	32
188	Genetic and environmental influences of white and gray matter signal contrast: A new phenotype for imaging genetics?. NeuroImage, 2012, 60, 1686-1695.	4.2	32
189	Multimodal Characterization of the Late Effects of Traumatic Brain Injury: A Methodological Overview of the Late Effects of Traumatic Brain Injury Project. Journal of Neurotrauma, 2018, 35, 1604-1619.	3.4	32
190	CoVA: An Acuity Score for Outpatient Screening that Predicts Coronavirus Disease 2019 Prognosis. Journal of Infectious Diseases, 2021, 223, 38-46.	4.0	31
191	Age does not increase rate of forgetting over weeks—Neuroanatomical volumes and visual memory across the adult life-span. Journal of the International Neuropsychological Society, 2005, 11, 2-15.	1.8	30
192	Entorhinal Cortex: Antemortem Cortical Thickness and Postmortem Neurofibrillary Tangles and Amyloid Pathology. American Journal of Neuroradiology, 2017, 38, 961-965.	2.4	30
193	Phase maps reveal cortical architecture. Proceedings of the National Academy of Sciences of the United States of America, 2007, 104, 11513-11514.	7.1	29
194	Target-specific contrast agents for magnetic resonance microscopy. Neurolmage, 2009, 46, 382-393.	4.2	29
195	PSACNN: Pulse sequence adaptive fast whole brain segmentation. NeuroImage, 2019, 199, 553-569.	4.2	29
196	Representational similarity precedes category selectivity in the developing ventral visual pathway. NeuroImage, 2019, 197, 565-574.	4.2	29
197	On Removing Interpolation and Resampling Artifacts in Rigid Image Registration. IEEE Transactions on Image Processing, 2013, 22, 816-827.	9.8	28
198	Event time analysis of longitudinal neuroimage data. NeuroImage, 2014, 97, 9-18.	4.2	28

#	Article	IF	CITATIONS
199	Functional density and edge maps: Characterizing functional architecture in individuals and improving cross-subject registration. NeuroImage, 2017, 158, 346-355.	4.2	28
200	Cortical surface registration using unsupervised learning. NeuroImage, 2020, 221, 117161.	4.2	26
201	A deep learning toolbox for automatic segmentation of subcortical limbic structures from MRI images. NeuroImage, 2021, 244, 118610.	4.2	26
202	Joint registration and synthesis using a probabilistic model for alignment of MRI and histological sections. Medical Image Analysis, 2018, 50, 127-144.	11.6	25
203	Microstructural parcellation of the human brain. NeuroImage, 2018, 182, 219-231.	4.2	24
204	Differential Regional Distribution of Juxtacortical White Matter Signal Abnormalities in Aging and Alzheimer's Disease. Journal of Alzheimer's Disease, 2017, 57, 293-303.	2.6	23
205	Automated MRI parcellation of the frontal lobe. Human Brain Mapping, 2014, 35, 2009-2026.	3.6	22
206	Entorhinal verrucae geometry is coincident and correlates with Alzheimer's lesions: a combined neuropathology and high-resolution ex vivo MRI analysis. Acta Neuropathologica, 2012, 123, 85-96.	7.7	21
207	Factors influencing accuracy of cortical thickness in the diagnosis of Alzheimer's disease. Human Brain Mapping, 2018, 39, 1500-1515.	3.6	21
208	Medial temporal cortices in ex vivo magnetic resonance imaging. Journal of Comparative Neurology, 2013, 521, 4177-4188.	1.6	20
209	Relevant feature set estimation with a knock-out strategy and random forests. NeuroImage, 2015, 122, 131-148.	4.2	20
210	The Ansa Subthalamica: A Neglected Fiber Tract. Movement Disorders, 2020, 35, 75-80.	3.9	20
211	Topological Correction of Subcortical Segmentation. Lecture Notes in Computer Science, 2003, , 695-702.	1.3	19
212	Multivariate statistical analysis of diffusion imaging parameters using partial least squares: Application to white matter variations in Alzheimer's disease. NeuroImage, 2016, 134, 573-586.	4.2	19
213	Shape Analysis with Overcomplete Spherical Wavelets. Lecture Notes in Computer Science, 2008, 11, 468-476.	1.3	19
214	Model-Based Segmentation of Hippocampal Subfields in Ultra-High Resolution In Vivo MRI. Lecture Notes in Computer Science, 2008, 11, 235-243.	1.3	19
215	Mid-space-independent deformable image registration. NeuroImage, 2017, 152, 158-170.	4.2	18
216	Optimizing the accuracy of cortical volumetric analysis in traumatic brain injury. MethodsX, 2020, 7, 100994.	1.6	18

#	Article	IF	CITATIONS
217	Discriminative Analysis for Image-Based Studies. Lecture Notes in Computer Science, 2002, , 508-515.	1.3	18
218	Example-Based Restoration of High-Resolution Magnetic Resonance Image Acquisitions. Lecture Notes in Computer Science, 2013, 16, 131-138.	1.3	18
219	The functional and structural significance of the frontal shift in the old/new ERP effect. Brain Research, 2006, 1081, 156-170.	2.2	17
220	Genetic influences on hippocampal volume differ as a function of testosterone level in middle-aged men. Neurolmage, 2012, 59, 1123-1131.	4.2	17
221	An algorithm for optimal fusion of atlases with different labeling protocols. NeuroImage, 2015, 106, 451-463.	4.2	16
222	En face speckle reduction in optical coherence microscopy by frequency compounding. Optics Letters, 2016, 41, 1925.	3.3	15
223	Quantification of structural brain connectivity via a conductance model. NeuroImage, 2019, 189, 485-496.	4.2	15
224	Cortical Folding Development Study based on Over-Complete Spherical Wavelets. , 2007, 2007, .		14
225	Improving the characterization of ex vivo human brain optical properties using high numerical aperture optical coherence tomography by spatially constraining the confocal parameters. Neurophotonics, 2020, 7, 045005.	3.3	14
226	Volumetric and fiber-tracing MRI methods for gray and white matter. Handbook of Clinical Neurology / Edited By P J Vinken and G W Bruyn, 2016, 135, 39-60.	1.8	13
227	Regionally specific TSC1 and TSC2 gene expression in tuberous sclerosis complex. Scientific Reports, 2018, 8, 13373.	3.3	13
228	Colocalization of neurons in optical coherence microscopy and Nissl-stained histology in Brodmann's area 32 and area 21. Brain Structure and Function, 2019, 224, 351-362.	2.3	13
229	Multimodal Image Registration Through Simultaneous Segmentation. IEEE Signal Processing Letters, 2017, 24, 1661-1665.	3.6	12
230	Maturational Changes in Human Dorsal and Ventral Visual Networks. Cerebral Cortex, 2019, 29, 5131-5149.	2.9	12
231	Active Contours Under Topology Control Genus Preserving Level Sets. Lecture Notes in Computer Science, 2005, , 135-145.	1.3	12
232	White matter abnormalities and cognition in patients with conflicting diagnoses and CSF profiles. Neurology, 2018, 90, e1461-e1469.	1.1	11
233	High-fidelity approximation of grid- and shell-based sampling schemes from undersampled DSI using compressed sensing: Post mortem validation. NeuroImage, 2021, 244, 118621.	4.2	11
234	Automatic segmentation of the structures in the human brain. NeuroImage, 2001, 13, 118.	4.2	10

#	Article	IF	CITATIONS
235	Reliability and sensitivity of two whole-brain segmentation approaches included in FreeSurfer – ASEG and SAMSEG. NeuroImage, 2021, 237, 118113.	4.2	10
236	Effects of Registration Regularization and Atlas Sharpness on Segmentation Accuracy. , 2007, 10, 683-691.		10
237	Pulse Sequence Resilient Fast Brain Segmentation. Lecture Notes in Computer Science, 2018, , 654-662.	1.3	9
238	Entorhinal Subfield Vulnerability to Neurofibrillary Tangles in Aging and the Preclinical Stage of Alzheimer's Disease. Journal of Alzheimer's Disease, 2022, 87, 1379-1399.	2.6	9
239	Avoiding symmetry-breaking spatial non-uniformity in deformable image registration via a quasi-volume-preserving constraint. NeuroImage, 2015, 106, 238-251.	4.2	8
240	Comprehensive cellularâ€resolution atlas of the adult human brain. Journal of Comparative Neurology, 2016, 524, Spc1.	1.6	8
241	Multi-Atlas Image Soft Segmentation via Computation of the Expected Label Value. IEEE Transactions on Medical Imaging, 2021, 40, 1702-1710.	8.9	8
242	Compensatory Brain Connection Discovery in Alzheimer's Disease. , 2020, 2020, 283-287.		7
243	Conductance-Based Structural Brain Connectivity in Aging and Dementia. Brain Connectivity, 2021, 11, 566-583.	1.7	7
244	Quantification of volumetric morphometry and optical property in the cortex of human cerebellum at micrometer resolution. NeuroImage, 2021, 244, 118627.	4.2	7
245	FreeSurfer is useful for early detection of Rasmussen's encephalitis prior to obvious atrophy. Developmental Medicine and Child Neurology, 2016, 58, 209-210.	2.1	6
246	Supervised Nonparametric Image Parcellation. Lecture Notes in Computer Science, 2009, 12, 1075-1083.	1.3	6
247	Task-Optimal Registration Cost Functions. Lecture Notes in Computer Science, 2009, 12, 598-606.	1.3	6
248	Chapter 52 Aids to telemetry in the presurgical evaluation of epilepsy patients: MRI, MEG and other non-invasive imaging techniques. Supplements To Clinical Neurophysiology, 2004, 57, 494-502.	2.1	5
249	What Data to Co-register for Computing Atlases. , 2007, 2007, .		5
250	Symmetric non-rigid image registration via an adaptive quasi-volume-preserving constraint. , 2013, 2013, 230-233.		5
251	Multiâ€modal robust inverse onsistent linear registration. Human Brain Mapping, 2015, 36, 1365-1380.	3.6	5
252	Detecting Structural Brain Connectivity Differences in Dementia Through a Conductance Model. , 2019, , .		5

#	Article	IF	CITATIONS
253	Hierarchical Clustering of Tractography Streamlines Based on Anatomical Similarity. Lecture Notes in Computer Science, 2016, , 184-191.	1.3	5
254	Geometry Driven Volumetric Registration. Lecture Notes in Computer Science, 2007, 20, 675-686.	1.3	5
255	Robust joint registration of multiple stains and MRI for multimodal 3D histology reconstruction: Application to the Allen human brain atlas. Medical Image Analysis, 2022, 75, 102265.	11.6	5
256	Scalable mapping of myelin and neuron density in the human brain with micrometer resolution. Scientific Reports, 2022, 12, 363.	3.3	5
257	Expected Label Value Computation for Atlas-Based Image Segmentation. , 2019, 2019, 334-338.		4
258	Learning Mri Contrast-Agnostic Registration. , 2021, , .		4
259	A Fast Approach to Automatic Detection of Brain Lesions. Lecture Notes in Computer Science, 2016, 10154, 52-61.	1.3	4
260	A novel algorithm for multiplicative speckle noise reduction in ex vivo human brain OCT images. NeuroImage, 2022, 257, 119304.	4.2	4
261	Long-Term Effects of Repeated Blast Exposure in United States Special Operations Forces Personnel: A Pilot Study Protocol. Journal of Neurotrauma, 2022, 39, 1391-1407.	3.4	4
262	Cortical Surface Shape Analysis Based on Spherical Wavelet Transformation. , 2006, 2006, .		3
263	3D Reconstruction and Segmentation of Dissection Photographs for MRI-Free Neuropathology. Lecture Notes in Computer Science, 2020, , 204-214.	1.3	3
264	Nonparametric Mixture Models for Supervised Image Parcellation. , 2009, 12, 301-313.		3
265	Detecting Cortical Surface Regions in Structural MR Data. , 2007, , .		2
266	Entorhinal verrucae correlate with surface geometry. Translational Neuroscience, 2012, 3, .	1.4	2
267	Anatomical priors for global probabilistic diffusion tractography. , 2009, , .		1
268	Mid-Space-Independent Symmetric Data Term for Pairwise Deformable Image Registration. Lecture Notes in Computer Science, 2015, 9350, 263-271.	1.3	1
269	Estimating the Location of Brodmann Areas from Cortical Folding Patterns Using Histology and Ex Vivo MRI. , 2013, , 129-156.		1